Article:

Feng, P., Xu, C., Bai, J. et al. (4 more authors) (2022) A simple approach to achieving ultrasmall III-nitride microlight-emitting diodes with red emission. ACS Applied Electronic Materials, 4 (6). pp. 2581-3165. ISSN 2637-6113

https://doi.org/10.1021/acsaelm.2c00311

ACS APPLIED ELECTRONIC MATERIALS

pubs.acs.org/acsaelm Article

A Simple Approach to Achieving Ultrasmall III-Nitride Microlight-Emitting Diodes with Red Emission

Peng Feng,[+] Ce Xu,[+] Jie Bai,[+] Chenqi Zhu, Ian Farrer, Guillem Martinez de Arriba, and Tao Wang*

Cite This: https://doi.org/10.1021/acsaelm.2c00311 Read Online

ACCESS | Metrics & More | Article Recommendations

ABSTRACT: The microdisplays for augmented reality and visual reality require ultrasmall microlight-emitting diodes (μLEDs) with a dimension of ≤5 μm. Furthermore, the microdisplays also need three kinds of such μLEDs each emitting red, green, and blue emission. Currently, in addition to a great challenge for achieving ultrasmall μLEDs mainly based on III-nitride semiconductors, another fundamental barrier is due to extreme difficulty in growing III-nitride-based red LEDs. So far, there has not been any effective approach to obtain high indium content InGaN as an active region required for a red LED while maintaining high optical performance. In this paper, we have demonstrated a selective epitaxy growth approach on a template featuring microhole arrays. This allows us to not only obtain the natural formation of ultrasmall μLEDs but also achieve InGaN with enhanced indium content at an elevated growth temperature, at which it is impossible to obtain InGaN-based red LEDs on a standard planar surface. By means of this approach, we have demonstrated red μLEDs (at an emission wavelength of 642 nm) with a dimension of 2 μm, exhibiting a high luminance of 3.5 × 10^7 cd/m^2 and a peak external quantum efficiency of 1.75% measured in a wafer form (i.e., without any packaging to enhance an extraction efficiency). In contrast, an LED grown under identical growth conditions but on a standard planar surface shows green emission at 538 nm. This highlights that our approach provides a simple solution that can address the two major challenges mentioned above.

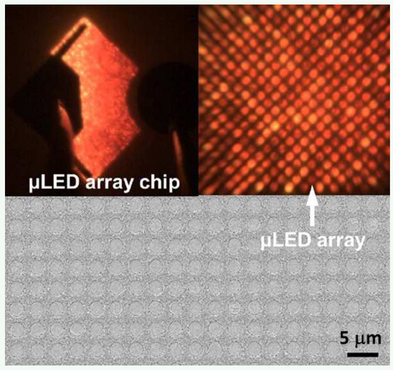

KEYWORDS: *InGaN, microLED, selective epitaxy growth, patterned template, MOVPE, EQE*

1. INTRODUCTION

There is a growing interest for developing microdisplays with compact screens of ≤1/4″ diagonal length, which have a wide range of applications in smart watches, smart phones, smart bands, and augmented reality and virtual reality (AR & VR) devices.[1−5] Their individual pixel elements typically consist of a large number of microscale visible LEDs mainly based on III-nitride semiconductors, which are referred to as microLEDs (μLEDs). For instance, the microdisplays for AR and VR require μLEDs with an ultrasmall dimension of ≤5 μm.[6−8] Such devices are typically utilized in a scenario where spaces are small or the devices need to be close to the eyes. Therefore, the devices require high resolution, high contrast ratio, high luminance, and high external quantum efficiency (EQE).[9,10] Of course, a microdisplay needs three kinds of individual μLEDs as a single pixel each emitting red, green, and blue emission (i.e., RGB), respectively.

InGaN semiconductors have direct bandgaps across their whole content ranging from 0.7 eV for InN to 3.43 eV for GaN, covering part of the infrared region, the full visible spectrum, and part of the ultraviolet (UV) region. So far, InGaN-based μLEDs with reasonably good performance in the blue and green spectral region have been reported. However, red LEDs still rely on AlGaInP materials. Although a large area AlGaInP red LED with a high efficiency of >50% can be obtained,[11] the efficiency reduces dramatically when its dimension is reduced to the microscale, namely, μLEDs. This is due to an enhancement in the surface recombination rate and the long diffusion lengths of carriers.[12−15] Moreover, the efficiency of AlGaInP red LEDs is sensitive to their junction temperature,[16,17] and thus, AlGaInP red LEDs generally suffer from a severe leakage current at a high temperature, generating a severe efficiency thermal drop. All these fundamental issues indicate that it is indispensable to develop III-nitride-based red LEDs to meet the requirements for the fabrication of a full color microdisplay.

InGaN with high indium content (>20%) is necessary for obtaining long wavelength emission. Unfortunately, it is greatly challenging to achieve high indium content InGaN while maintaining high optical performance.[18,19] A typical method to achieve high indium content in InGaN is to lower the growth

Received: March 9, 2022
Accepted: May 10, 2022

temperature for InGaN. However, it is clear that this method is not ideal because it causes a significant degradation in crystal quality.

In general, vapor−solid thermodynamic equilibrium can be modified by stress, making the solid-phase epitaxial composition reduce toward lattice-matched conditions. This is the major reason why it is difficult to increase indium incorporation into GaN.[20−24] Therefore, the growth of InGaN on a relaxed layer is beneficial for obtaining high indium content in InGaN. However, bear in mind that the formation of a relaxed layer is often associated with the generation of extra defects if a heterostructure with a large lattice mismatch is used to generate a relaxed layer. This leads to degradation in optical performance. Furthermore, the stress status of an underlying layer plays a critical role in determining indium incorporation into GaN. Generally speaking, tensile stress tends to enhance indium incorporation into GaN, offering a unique advantage for growing red LEDs on silicon substrates as GaN on Si suffering tensile stress.[25,26] In contrast, GaN grown on sapphire substrates exhibits compressive strain.

The growth of InGaN-based red LEDs has been reported by means of inserting a thin AlN or an AlGaN layer into each InGaN quantum well as an emitting region, leading to an enhancement in strain that pushes the emission wavelength of InGaN quantum wells toward longer wavelength.[27,28] So far, this approach has become a popular method for the growth of long wavelength emitters, in particular, red LEDs.[25−30] Furthermore, by combining the idea of inserting a thin AlN or AlGaN and further adjusting the in-plane strain of a GaN template by tuning the GaN thickness, 633 nm-wavelength red LEDs with an external quantum efficiency (EQE) of 1.6% has been reported, where an extremely thick GaN (8−10 μm) template has been employed.[26,29] A more recent work has demonstrated that a peak EQE as high as 4.5% has been achieved on red InGaN μLEDs.[31] However, it is worth noting that the approach of strain enhancing also leads to a reduction in internal quantum efficiency.

We expect that an enhanced relaxation can be achieved by using a selective epitaxy growth approach on a microhole-patterned template, which we have developed recently, where μLEDs can be naturally formed but without employing any dry-etching techniques because selective epitaxy growth can take place only within these microholes.[7,8] In this work, we are proposing to employ this approach to achieve ultrasmall red μLED arrays with enhanced quantum efficiency but without inserting any thin AlN or AlGaN into InGaN quantum wells as an emitting region. It is expected that no lateral confinement during the selective epitaxy growth process leads to strain relaxation effectively and naturally. By this mechanism, 642 nm red μLEDs with a dimension of 2 μm have been achieved by our selective epitaxy growth conducted at an elevated temperature, at which a red LED cannot be achieved on a standard planar GaN surface. The resultant external quantum efficiency is 1.75%. For comparison, only 538 nm green LEDs on a standard planar GaN template can be obtained even under identical growth conditions. Our X-ray diffraction measurements have confirmed that a significant enhancement in indium content in InGaN has been achieved by our approach.

2. RESULTS AND DISCUSSION

In this work, two different InGaN-based LED samples have been designed and then grown, aiming to study the influence of selective epitaxial growth on the optical performance of III-nitride LEDs grown on a prepatterned template featuring microhole arrays. A μLED array sample is obtained by our selective epitaxy growth on the prepatterned n-GaN template as mentioned above and is denoted as LED A. The other one is a normal LED sample grown under identical growth but on a standard planar n-GaN template without any features and is denoted as LED B.

Silicon-doped n-GaN epiwafers are first grown on *c*-plane (0001) sapphire substrates using the standard two-step approach by a metalorganic vapor phase epitaxy (MOVPE) technique. Initially, a 25 nm GaN nucleation layer is prepared at a low temperature after the substrate is subject to a thermally annealing process at a high temperature of 1150 °C, followed by a 1 μm GaN buffer layer, and then another 500 nm silicon-doped n-GaN layer both grown at a high temperature of 1120 °C. For LED A, the n-GaN template is further patterned into microhole arrays using SiO_2 masks on its top, which is then used as a prepatterned template for our selective epitaxial growth.

Figure 1a shows the schematics of our selective epitaxy growth approach, allowing us to naturally achieve μLED arrays

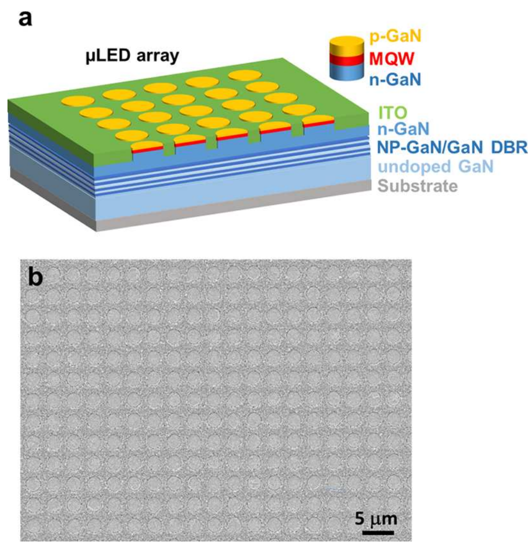

Figure 1. (a) Schematic of selective epitaxy growth and (b) plan-view SEM image for the μLED array epiwafer, showing a diameter of 2 μm and an interpitch of 1.5 μm.

without involving any dry-etching process, i.e., LED A. For the detailed information on fabricating the prepatterned templates, refer to the Experimental Methods section.

Afterward, a standard III-nitride LED structure is selectively grown on the micropatterned template by MOVPE, namely, a silicon-doped n-GaN layer is first prepared, followed by an $In_{0.05}Ga_{0.95}N$/GaN superlattice (SLS) structure as a prelayer, five periods of InGaN/GaN multiple quantum wells (MQWs) as an emitting region, then a 20 nm *p*-type $Al_{0.2}Ga_{0.8}N$ as an electron blocking layer, and a final 150 nm *p*-type GaN layer. The total thickness of the overgrown layers is 500 nm, which matches the thickness of the SiO_2 masks. Due to the SiO_2 masks, the growth of the LED structure takes place within the microholes only, naturally forming regularly arrayed μLEDs.

A Raith 150 scanning electron microscopy (SEM) system has been used to characterize the surface morphology of our regularly arrayed μLEDs. Figure 1b shows a typical plan-view

https://doi.org/10.1021/acsaelm.2c00311
ACS Appl. Electron. Mater. XXXX, XXX, XXX−XXX

SEM image of our regularly arrayed μLEDs wafer (i.e., LED A), exhibiting a nice circular shape with an excellent high uniformity in shape, diameter, and interpitch. All μLEDs are 2 μm in diameter and only 1.5 μm in interpitch. Such a small diameter and an interpitch are crucial for manufacturing a high-resolution microdisplay in a compact manner. Furthermore, the μLED pixels share a common *n* contact while all the *p* contacts are left open. As a result, our regularly arrayed μLED epiwafers well match any existing manufacturing technique of microdisplays, for instance, the pick-and-place technology, which has been widely used,[32] and the integrating technique using driving transistors based on the silicon CMOS IC to achieve individually addressable μLED-based microdisplays.[33]

A high-resolution X-ray diffractometer (HRXRD) (Bruker D8) has been employed to determine the indium content of the InGaN MQWs by performing ω-2θ scan measurements along the (002) direction, together with a fitting using the Bruker JV-RADS simulation software. Figure 2a,b shows the

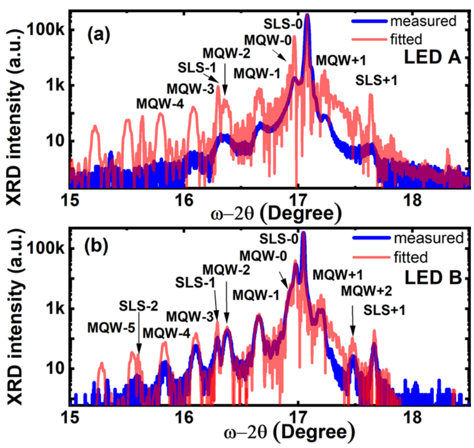

Figure 2. HRXRD ω-2θ scan curves of the μLED array sample on a patterned template, i.e., (a) LED A, and the LED sample grown on a standard planar template, i.e., (b) LED B under identical conditions. Fittings have also been provided to determine the indium content in InGaN MQWs.

HRXRD ω-2θ scan curves of our regularly arrayed μLED wafer (i.e., LED A) and the standard LED wafer (i.e., LED B), respectively. In both cases, the satellite peaks with up to 4 or 5 orders from the InGaN/GaN MQWs have been clearly observed. The satellite peaks from the SLS structure as a prelayer have also been observed. Based on a detailed fitting, it can be determined that the indium content of the InGaN MQWs of LED A is 31% and that the thicknesses of the InGaN quantum well and the barrier are 2.2 and 13.8 nm, respectively. In contrast, LED B exhibits 24% indium content in the InGaN MQWs with a 2.6 nm quantum well and a 14.1 nm barrier. The XRD fittings are conducted based on fully strained InGaN MQWs for both LEDs. It is well known that strain relaxation will reduce the strain-induced quantum-confined Stark effect (QCSE), leading to a blue-shift in the emission. It means that if the InGaN MQWs are assumed to be strain-relaxed, the indium content should be even higher. In consideration of a higher chance of strain relaxation for the μLEDs, the fitted values of indium contents represent the least difference between the two LEDs. This direct comparison indicates that enhanced indium content in InGaN MQWs can be obtained by using our selective epitaxy growth approach on a prepatterned template featuring microhole arrays.

Finally, both the regularly arrayed μLED wafer (i.e., LED A) and the standard LED wafer (i.e., LED B) have been fabricated into LED devices with an area of 330 × 330 μm^2. For the detailed information about device fabrication, refer to the Experimental Methods section. For LED A, each LED device consists of a few thousands of 2 μm μLEDs connected. In this work, the μLEDs in LED A share a common *p* contact and *n* contact, which are driven simultaneously in all electroluminescence (EL) measurements. However, it is worth noting that our arrayed μLEDs are designed to make the *p* contacts of each μLED left open, providing an opportunity in the future to allow indium bumps to be bonded to an active matrix driving transistors. This means that our regularly arrayed μLED structure entirely matches any existing individually addressable μLED microdisplays.

For a direct comparison, the LED B wafer has also been processed under identical conditions in the same batch. All the characteristics of our μLED chips in the present study have been carried out on bare chips, meaning that we did not use coating or passivation or epoxy or reflector for improving extraction efficiency. Current−voltage (*I*−*V*) characteristic and EL measurements have been performed at room temperature in continuous wave (CW) mode using a Keithley 2400 sourcemeter on a probe station equipped with an optical microscopy system.

The EL spectra have been measured on the two LED devices under identical conditions aiming to make a direct comparison. For instance, Figure 3a,b shows the EL spectra of the two LED devices measured at a current density of 10 A/cm^2, respectively. Both spectra exhibit a single emission peak. The

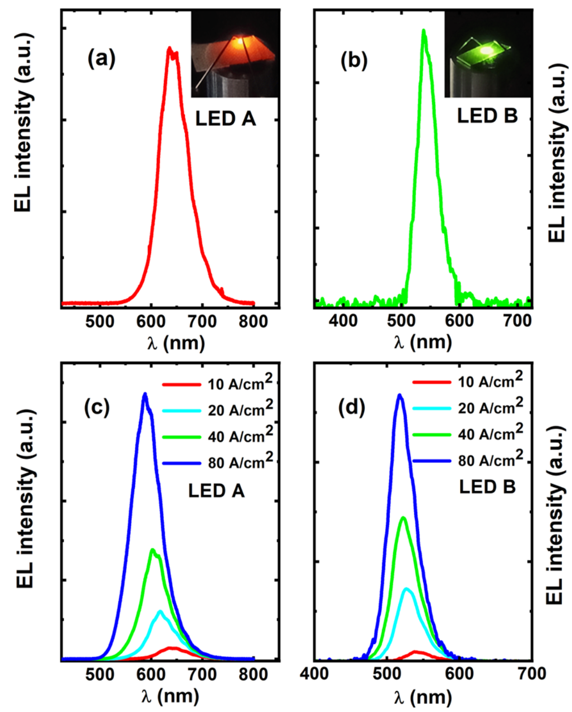

Figure 3. EL spectra measured at 10 A/cm^2 for the μLED array device, i.e., (a) LED A and (b) LED B, where the insets show their respective emission images. EL spectra measured at increased current densities from 10 to 80 A/cm^2 for (c) LED A and (d) LED B, respectively.

https://doi.org/10.1021/acsaelm.2c00311
ACS Appl. Electron. Mater. XXXX, XXX, XXX−XXX

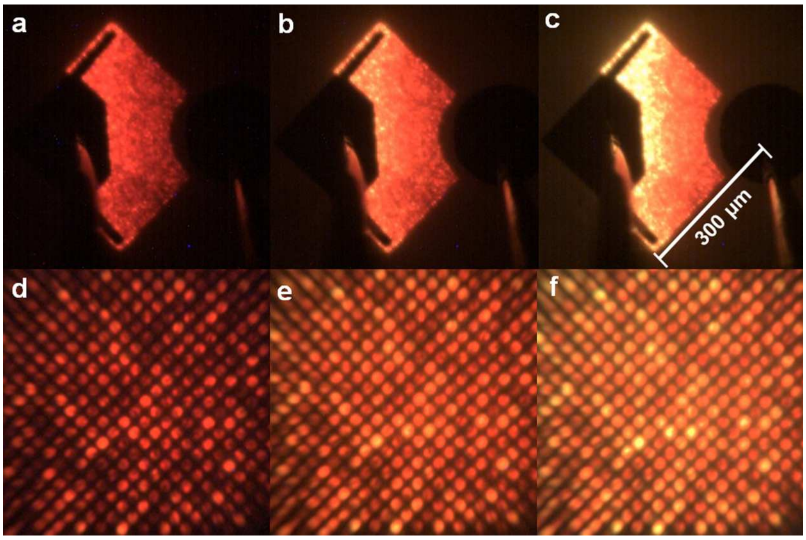

Figure 4. Emission images of the μLED array device taken using an optical microscopy system as a function of injection current density (4, 8, and 12 A/cm^2) under (a−c) a low magnification and (d−f) a high magnification, respectively.

μLED array device shows a strong emission at an emission wavelength of 642 nm in the red spectral region. The inset of Figure 3a exhibits an emission image of the μLED array chip, demonstrating red light. In contrast, Figure 3b displays a strong green emission at 538 nm from the LED B device also measured at 10 A/cm^2, and the inset displays its emission image. This means that the selective epitaxial growth on a prepatterned template featuring regularly arrayed microholes results in a red-shift of about 100 nm in emission wavelength in comparison with the LED grown on a standard planar GaN surface, although both are grown under identical growth conditions. As discussed earlier, the growth of InGaN on a relaxed layer is beneficial for obtaining high indium content in InGaN. Due to no lateral confinement during the overgrowth within the microholes, the overgrown n-GaN is very likely strain-relaxed, which leads to an enhancement in the indium content in the overlying InGaN MQWs. Combined with the XRD results, it has been confirmed that our selective epitaxy growth approach can enhance indium incorporation into GaN significantly. Figure 3c,d shows the EL spectra of LED A and LED B, both measured as a function of injection current density ranging from 10 to 80 A/cm^2, respectively.

In order to demonstrate emitting μLED pixels, optical microscopy images have been taken using a micro-EL measurement system where emissions are collected through two objective lenses (one 10× magnification lens with NA = 0.28 and another 50× magnification lens with NA = 0.43). Figure 4a−c displays the emission images of our μLED array chip taken under 4, 8, and 12 A/cm^2 current density, respectively, while Figure 4d−f provides their corresponding emission images taken under a high magnification, showing strong red emissions from individual 2 μm μLED pixels even under low current densities. It is worth mentioning that such low current densities used for the operation of our μLEDs are lower than a typical current density (22 A/cm^2) for the operation of a conventional broad area LED.

Both light output powers and luminous flux have been measured on the bare-chip LEDs bonded on TO5-headers in CW mode using a LCS-100 integrating sphere equipped with a CCD APRAR spectrometer. Figure 5a−c shows the output power, luminance, and EQE of the μLED array device (i.e.,

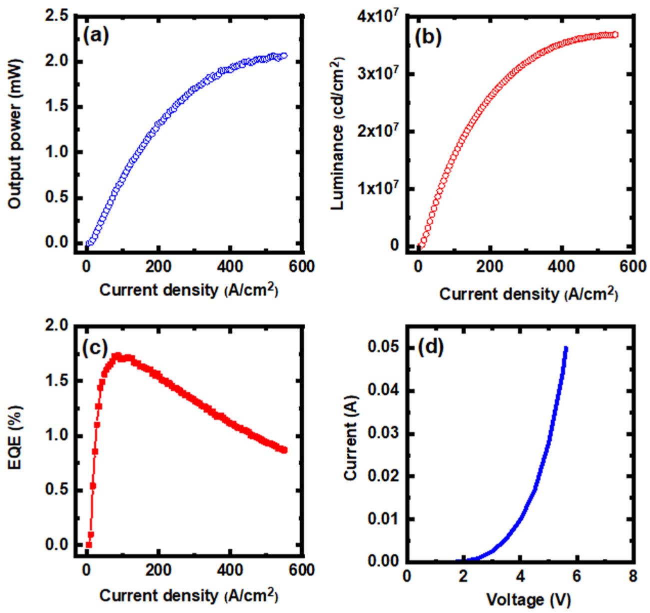

Figure 5. (a) Output power, (b) luminance, (c) EQE, and (d) current−voltage characteristics of the μLED array device (i.e., LED A).

LED A) as a function of injection current density. This demonstrates that the output power and luminescence increase monolithically with increasing current density up to 450 A/cm^2 and that a high luminance of 3.5 × 10^7 cd/m^2 has been achieved. The peak EQE is about 1.75%. It is worth highlighting that although there are not any heat-sink components used, our ultrasmall μLEDs can still sustain a high current density of above 450 A/cm^2, also confirming the high crystal quality of our μLED array sample achieved by our selective epitaxy growth approach. Figure 5d displays the typical I−V characteristics of LED A measured as a function of bias, which is similar to that of the LED B device. This also shows the good electrical property of our μLED array device.

https://doi.org/10.1021/acsaelm.2c00311
ACS Appl. Electron. Mater. XXXX, XXX, XXX−XXX

3. CONCLUSIONS

In summary, we are proposing to employ a selective epitaxy growth approach on a microhole patterned template to significantly enhance strain relaxation, allowing us to not only obtain the natural formation of regularly arrayed μLEDs but also achieve enhanced indium content in the InGaN/GaN MQWs used as an active region for the μLEDs. By means of this approach, we have demonstrated red InGaN-based μLED arrays with a dimension of 2 μm and an interpitch of 1.5 μm. A high luminance of 3.5×10^7 cd/m^2 and a peak EQE of 1.7% have been achieved for the red μLED array chip in a wafer form without any packaging. In contrast, the standard LED grown under growth conditions but on a standard planar GaN template demonstrates green emission. This means that our approach paves the way for achieving long wavelength InGaN-based μLEDs with ultrasmall dimensions at an elevated growth temperature, at which it is impossible to obtain InGaN-based red LEDs on a standard planar template.

4. EXPERIMENTAL METHODS

4.1. Fabrication of Prepatterned Templates. A 500 nm SiO_2 dielectric film is deposited on the n-GaN template by a plasma-enhanced chemical vapor deposition (PECVD) technique, followed by employing a standard photolithography and then a dry etching technique to selectively etch the SiO_2 dielectric layer down to the n-GaN surface by inductively coupled plasma (ICP), forming regularly arrayed microholes with a diameter of 2 μm and an interpitch of 1.5 μm. This prepatterned template will then be used for further selective epitaxy growth. Finally, μLEDs will be selectively grown only within SiO_2 microhole regions, naturally forming regularly arrayed μLEDs.

4.2. Device Fabrication. Indium-tin-oxide (ITO) is deposited and then undergoes an annealing process in air at 600 °C for 1 min, forming transparent *p*-type contact, while Ti/Al/Ni/Au alloys are prepared as *n*-type contact. Ti/Au alloys are used as *p*-type and *n*-type electrodes. All the characteristics of the LEDs in this paper are conducted on bare chips, namely, no coating, no passivation, no epoxy, or no reflector, which are often employed for obtaining enhanced extraction efficiency.

AUTHOR INFORMATION

Corresponding Author

Tao Wang − *Department of Electronic and Electrical Engineering, The University of Sheffield, Sheffield S1 3JD, United Kingdom*; orcid.org/0000-0001-5976-4994; Email: t.wang@sheffield.ac.uk

Authors

Peng Feng − *Department of Electronic and Electrical Engineering, The University of Sheffield, Sheffield S1 3JD, United Kingdom*

Ce Xu − *Department of Electronic and Electrical Engineering, The University of Sheffield, Sheffield S1 3JD, United Kingdom*

Jie Bai − *Department of Electronic and Electrical Engineering, The University of Sheffield, Sheffield S1 3JD, United Kingdom*

Chenqi Zhu − *Department of Electronic and Electrical Engineering, The University of Sheffield, Sheffield S1 3JD, United Kingdom*

Ian Farrer − *Department of Electronic and Electrical Engineering, The University of Sheffield, Sheffield S1 3JD, United Kingdom*

Guillem Martinez de Arriba − *Department of Electronic and Electrical Engineering, The University of Sheffield, Sheffield S1 3JD, United Kingdom*

Complete contact information is available at: https://pubs.acs.org/10.1021/acsaelm.2c00311

Author Contributions

[+]P.F., C.X., and J.B. contributed equally to this work.

Author Contributions

T.W. conceived the idea and organized the project. T.W. and J.B. prepared the manuscript. P.F., X.C., and C.Z. grew all the samples. P.F., X.C., and I.F. performed the material characterization. J.B. and G.M.D.A. fabricated the prepatterned templates and carried out the device fabrication. J.B. conducted the device characterization.

Notes

The authors declare no competing financial interest.

ACKNOWLEDGMENTS

Financial support from the Engineering and Physical Sciences Research Council (EPSRC), UK via EP/P006973/1, EP/M015181/1, and EP/P006361/1 is acknowledged.

REFERENCES

(1) Meng, W.; Xu, F.; Yu, Z.; Tao, T.; Shao, L.; Liu, L.; Li, T.; Wen, K.; Wang, J.; He, L.; Sun, L.; Li, W.; Ning, H.; Dai, N.; Qin, F.; Tu, X.; Pan, D.; He, S.; Li, D.; Zheng, Y.; Lu, Y.; Liu, B.; Zhang, R.; Shi, Y.; Wang, X. Three-dimensional Monolithic Micro-LED Display Driven by Atomically Thin Transistor matrix. *Nat. Nanotechnol.* **2021**, *16*, 1231.

(2) Park, J.; Choi, J. H.; Kong, K.; Han, J. H.; Park, J. H.; Kim, N.; Lee, E.; Kim, D.; Ki, J.; Chung, D.; Jun, S.; Kim, M.; Yoon, E.; Shin, J.; Hwang, S. Electrically Driven Mid-Submicrometre Pixelation of InGaN Micro-Light-Emitting Diode Displays for Augmented-Reality Glasses. *Nat. Photonics* **2021**, *15*, 449.

(3) Huang, Y.; Hsiang, E.-L.; Deng, M.-Y.; Wu, S.-T. Mini-LED, Micro-LED and OLED Displays: Present Status and Future Perspectives. *Light: Sci. Appl.* **2020**, *9*, 105.

(4) Han, H.-V.; Lin, H.-Y.; Lin, C.-C.; Chong, W.-C.; Li, J.-R.; Chen, K.-J.; Chen, T.-M.; Chen, H.-M.; Lau, K.-M.; Kuo, H.-C. Resonant-enhanced full-Color Emission of Quantum-Dot-Based Micro LED Display Technology. *Opt. Express* **2015**, *23*, 32504−32515.

(5) Green, R. P.; McKendry, J. J. D.; Massoubre, D.; Gu, E.; Dawson, M. D.; Kelly, A. E. Modulation Bandwidth Studies of recombination Processes in Blue and Green InGaN Quantum Well Micro-Light-Emitting Diodes. *Appl. Phys. Lett.* **2013**, *102*, No. 091103.

(6) Ley, R. T.; Smith, J. M.; Wong, M. S.; Margalith, T.; Nakamura, S.; DenBaars, S. P.; Gordon, M. J. Revealing the Importance of Light Extraction Efficiency in InGaN/GaN MicroLEDs via Chemical Treatment and Dielectric Passivation. *Appl. Phys. Lett.* **2020**, *116*, 251104.

(7) Bai, J.; Cai, Y.; Feng, P.; Fletcher, P.; Zhao, X.; Zhu, C.; Wang, T. A Direct Epitaxial Approach To Achieving Ultrasmall and Ultrabright InGaN Micro Light-Emitting Diodes (μLEDs). *ACS Photonics* **2020**, *7*, 411.

(8) Bai, J.; Cai, Y.; Feng, P.; Fletcher, P.; Zhu, C.; Tian, Y.; Wang, T. Ultrasmall, Ultracompact and Ultrahigh Efficient InGaN Micro Light Emitting Diodes (μLEDs) with Narrow Spectral Line Width. *ACS Nano* **2020**, *14*, 6906.

(9) Zhan, T.; Yin, K.; Xiong, J.; He, Z.; Wu, S.-T. Augmented Reality and Virtual Reality Displays: Perspectives and Challenges. *iScience* **2020**, *23*, No. 101397.

(10) Liu, Z.; Lin, C.-H.; Hyun, B.-R.; Sher, C.-W.; Luo, B.; Lv, Z.; Jiang, F.; Wu, T.; Ho, C.-H.; Kuo, H.-C.; He, J.-H. Micro-light-emitting diodes with quantum dots in display technology. *Light: Sci. Appl.* **2020**, *9*, 83.

(11) Krames, M. R.; Ochiai-Holcomb, M.; Höfler, G. E.; Carter-Coman, C.; Chen, E. I.; Tan, I. H.; Grillot, P.; Gardner, N. F.; Chui, H. C.; Huang, J. W.; Stockman, S. A.; Kish, F. A.; Craford, M. G.;

Tan, T. S.; Kocot, C. P.; Hueschen, M.; Posselt, J.; Loh, B.; Sasser, G.; Collins, D. High-Power Truncated-Inverted-Pyramid $(Al_xGa_{1-x})_{0.5}In_{0.5}P/GaP$ Light-Emitting Diodes Exhibiting >50% External quantum efficiency. *Appl. Phys. Lett.* **1999**, *75*, 2365−2367.

(12) Boroditsky, M.; Gontijo, I.; Jackson, M.; Vrijen, R.; Yablonovitch, E.; Krauss, T.; Cheng, C. C.; Scherer, A.; Bhat, R.; Krames, M. Surface Recombination Measurements on III−V Candidate Materials for Nanostructure Light-Emitting Diodes. *J. Appl. Phys.* **2000**, *87*, 3497.

(13) Royo, P.; Stanley, R. P.; Ilegems, M.; Streubel, K.; Gulden, K. H. Experimental Determination of the Internal Quantum Efficiency of AlGaInP Microcavity Light-Emitting Diodes. *J. Appl. Phys.* **2002**, *91*, 2563.

(14) Oh, J.-T.; Lee, S.-Y.; Moon, Y.-T.; Moon, J. H.; Park, S.; Hong, K. Y.; Song, K. Y.; Oh, C.; Shim, J.-I.; Jeong, H.-H.; Song, J.-O.; Amano, H.; Seong, T.-Y. Light Output Performance of Red AlGaInP-Based Light Emitting Diodes with Different Chip Geometries and Structures. *Opt. Express* **2018**, *26*, 11194.

(15) Wong, M. S.; Kearns, J. A.; Lee, C.; Smith, J. M.; Lynsky, C.; Lheureux, G.; Choi, H.; Kim, J.; Kim, C.; Nakamura, S.; Speck, J. S.; Denbaars, S. P. Improved Performance of AlGaInP Red Micro-Light-Emitting Diodes with Sidewall Treatments. *Opt. Express* **2020**, *28*, 5787−5793.

(16) Yadav, A.; Titkov, I. E.; Sokolovskii, G. S.; Karpov, S. Y.; Dudelev, V. V.; Soboleva, K. K.; Strassburg, M.; Pietzonka, I.; Lugauer, H.-J.; Rafailo, E. U. Temperature Effects on Optical Properties and Efficiency of Red AlGaInP-Based Light Emitting Diodes under High Current Pulse Pumping. *J. Appl. Phys.* **2018**, *124*, No. 013103.

(17) Oh, C.-H.; Shim, J.-I.; Shin, D.-S. Current- and Temperature-Dependent Efficiency Droops in InGaN-Based Blue and AlGaInP-Based Red Light-Emitting Diodes. Japanese. *J. Appl. Phys.* **2019**, *58*, SCCC08.

(18) El-Masry, N. A.; Piner, E. L.; Liu, S. X.; Bedair, S. M. Phase Separation in InGaN Grown by Metalorganic Chemical Vapor Deposition. *Appl. Phys. Lett.* **1998**, *72*, 40.

(19) Wakahara, A.; Tokuda, T.; Dang, X.-Z.; Noda, S.; Sasaki, A. Compositional Inhomogeneity and Immiscibility of a GaInN Ternary Alloy. *Appl. Phys. Lett.* **1997**, *71*, 906−908.

(20) Inatomi, Y.; Kanagawa, Y.; Ito, T.; Suski, T. Theoretical Study of the Composition Pulling Effect in InGaN Metalorganic Vapor-Phase Epitaxy Growth. *Jpn. J. Appl. Phys.* **2017**, *56*, No. 078003.

(21) Wang, T. Topical Review: Development of Overgrown Semipolar GaN for High Efficiency Green/Yellow Emission. *Semicond. Sci. Technol.* **2016**, *31*, No. 093003.

(22) Pereira, S.; Correia, M. R.; Pereira, E.; O'Donnell, K. P.; Alves, E.; Sequeira, A. D.; Franco, N.; Watson, I. M.; Deatcher, C. J. Strain and Composition Distributions in Wurtzite InGaN/GaN Layers Extracted from X-ray Reciprocal Space Mapping. *Appl. Phys. Lett.* **2002**, *80*, 3913.

(23) Shimizu, M.; Kawaguchi, Y.; Hiramatsu, K.; Sawaki, N. Metalorganic Vapor Phase Epitaxy of Thick InGaN on Sapphire Substrate. *Jpn. J. Appl. Phys., Part 1* **1997**, *36*, 3381.

(24) Sonderegger, S.; Feltin, E.; Merano, M.; Crottini, A.; Carlin, J. F.; Sachot, R.; Deveaud, B.; Grandjean, N.; Ganière, J. D. High Spatial Resolution Picosecond Cathodoluminescence of InGaN Quantum Wells. *Appl. Phys. Lett.* **2006**, *89*, 232109.

(25) Tawfik, W. Z.; Hyun, G. Y.; Ryu, S.-W.; Ha, J. S.; Lee, J. K. Piezoelectric Field in Highly Stressed GaN-Based LED on Si (1 1 1) Substrate. *Opt. Mater.* **2016**, *55*, 17−21.

(26) Iida, D.; Zhuang, Z.; Kirilenko, P.; Velazquez-Rizo, M.; Najmi, M. A.; Ohkawaa, K. High-color-Rendering-Index Phosphor-Free InGaN-Based White Light-Emitting Diodes by Carrier Injection Enhancement via V-Pits. *Appl. Phys. Lett.* **2020**, *116*, 162101.

(27) Hwang, J.-I.; Hashimoto, R.; Saito, S.; Nunoue, S. Development of InGaN-Based Red LED Grown on (0001) Polar Surface. *Appl. Phys. Express* **2014**, *7*, No. 071003.

(28) Hashimoto, R.; Hwang, J.; Saito, S.; Nunoue, S. High-Efficiency Yellow Light-Emitting Diodes Grown on Sapphire (0001) Substrates. *Phys. Status Solidi C* **2014**, *11*, 628.

(29) Zhuang, Z.; Iida, D.; Ohkawa, K. InGaN-based red light-emitting diodes: from traditional to micro-LEDs. *Jpn. J. Appl. Phys.* **2022**, *61*, SA0809.

(30) Li, P.; Li, H.; Zhang, H.; Lynsky, C.; Iza, M.; Speck, J. S.; Nakamura, S.; DenBaars, S. P. Size-Independent Peak External Quantum Efficiency (>2%) of InGaN Red Microlight-Emitting Diodes with An Emission Wavelength over 600 nm. *Appl. Phys. Lett.* **2021**, *119*, No. 081102.

(31) Li, P.; Li, H.; Zhang, H.; Yang, Y.; Wong, M. S.; Lynsky, C.; Iza, M.; Gordon, M. J.; Speck, J. S.; Nakamura, S.; DenBaars, S. P. Red InGaN micro-light-emitting diodes (>620 nm) with a peak external quantum efficiency of 4.5% using an epitaxial tunnel junction contact. *Appl. Phys. Lett.* **2022**, *120*, 121102.

(32) Wong, M. S.; Hwang, D.; Alhassan, A. I.; Lee, C.; Ley, R.; Nakamura, S.; DenBarrs, S. P. High efficiency of III-nitride micro-light emitting diodes by sidewall passivation using atomic layer deposition. *Opt. Express* **2018**, *26*, 21324−21331.

(33) Day, J.; Li, J.; Lie, D. Y. C.; Bradford, C.; Lin, J. Y.; Jiang, H. X. III-Nitride full-scale high-resolution microdisplays. *Appl. Phys. Lett.* **2011**, *99*, No. 031116.

https://doi.org/10.1021/acsaelm.2c00311
ACS Appl. Electron. Mater. XXXX, XXX, XXX−XXX